JOURNAL OF PROPULSION AND POWER
Vol. 12, No. 4, July–August 1996

Investigation of the Effect of Tabs on Supersonic Jets Using Advanced Diagnostics

M. F. Reeder,* M. Samimy,† and G. S. Elliott‡
Ohio State University, Columbus, Ohio 43210

The effect of tabs on supersonic jets has been assessed using two laser-based experimental techniques. In the first instance, visualizations of the mixing layer were obtained simultaneously from two orthogonal vantage points, yielding considerable insight into the characteristics of the mixing. Secondly, quantitative data were gathered using a filtered Rayleigh scattering (FRS) technique. Instantaneous images were collected for both techniques using a Nd:YAG pulsed laser and intensified charge-coupled device cameras. Average streamwise velocities were measured in isothermal Mach 1.0, 1.5, and 2.0 jets using FRS across the two-dimensional image field. When tabs were employed, the molecular scattering clearly showed the drastic deformation of the jet. From these images, quantitative data was derived that definitively identifies the presence of counter-rotating streamwise vortices generated by each tab.

Nomenclature

D = function describing the effect of Doppler shift, Eq. (5)
E = function describing changes in scattering spectra, Eq. (5)
f = frequency
$f(U)$ = function of streamwise velocity
$f(V)$ = function of lateral velocity
f_0 = incident frequency of the laser
I = light intensity within the jet
I_∞ = light intensity within the ambient air
k_s = scattered light wavevector
k_0 = incident light wavevector
$R^*(f)$ = function describing the Rayleigh scattering shape in the frequency domain
V = total velocity vector
Δf = frequency shift from the Doppler effect
θ = scattering angle
λ = laser wavelength
ρ = density within the jet
ρ^* = density ratio, ρ/ρ_∞
ρ_∞ = density within the ambient air

Introduction

MIXING plays an important role in jet flows, both in terms of noise generation and combustion characteristics. The nozzle configuration can play an important role in the evolution of a jet and its mixing properties. One simple way of manipulating a jet is to place tabs, small protrusions into the flow, at the nozzle exit plane.

Tabs that are small in comparison to the length scale of a nozzle have a substantial effect on both subsonic and supersonic jets.[1,2] In work preceding the present investigation, Samimy et al.[3] and Zaman et al.[4] established that an axisymmetric jet with two triangularly shaped delta tabs (Fig. 1) entrains substantially more ambient fluid than a jet without tabs. Using hot-wire anemometry in a subsonic jet, it was proven that each tab generates a set of counter-rotating streamwise vortices that act to entrain additional ambient fluid. The production of streamwise vortices by tabs was confirmed by laser Doppler velocimetry (LDV) measurements performed in a water tunnel.[5,6] The circulation of the streamwise vortex pattern generated by two tabs and the resultant deformation of the jet is shown in Fig. 2.

Considering the flow visualizations and analytical arguments elucidated by Zaman et al.,[4] it is apparent that the pattern of streamwise vorticity is present not only in subsonic, but also supersonic jets. However, prior to the present work, this assertion had not been experimentally verified in supersonic jets. This is partly because of the fact that many intrusive diagnostics commonly used in subsonic flows are problematic in the supersonic regime. This familiar dilemma has spawned a great deal of research into laser-based diagnostics for high-speed flows.

Among the most well-developed approaches is LDV, but the point-by-point nature of the measurements is often undesirable for global measurements in high-speed flow facilities. Particle imaging velocimetry (PIV), a more recent technique that relies on the time-of flight of particles in the flow, permits velocity measurements across a plane but, like LDV, requires that the flow be seeded. Yet another approach to diagnostics across a planar region is to determine the Doppler shift by considering the scattering process in molecular species which fluoresce for a given wavelength of incident light. Of course, for this technique to be successful, the species must either be present naturally or be artificially introduced into the flow.

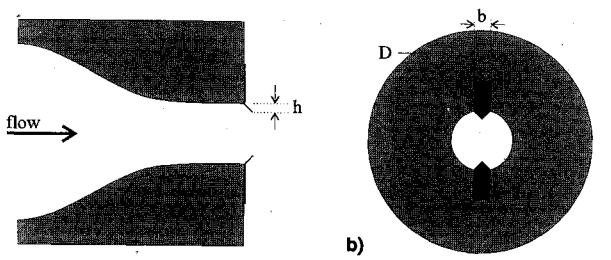

Fig. 1 Sketch of a nozzle with two delta tabs inserted at the exit as viewed from the a) side and b) front. The tab dimensions are $b = 0.28D$ and $h = 0.10D$, angle = 45 deg.

Presented as Paper 95-0672 at the AIAA 33rd Aerospace Sciences Meeting, Reno, NV, Jan. 9–12, 1995; received Sept. 8, 1995; revision received Feb. 15, 1996; accepted for publication March 1, 1996.

*Graduate Student, Department of Mechanical Engineering; currently National Research Council Fellow, NASA Lewis Research Center, Cleveland, OH. Member AIAA.

†Professor, Department of Mechanical Engineering. Associate Fellow AIAA.

‡Postdoctoral Researcher, Department of Mechanical Engineering; currently Assistant Professor, Rutgers University, New Brunswick, NJ. Member AIAA.

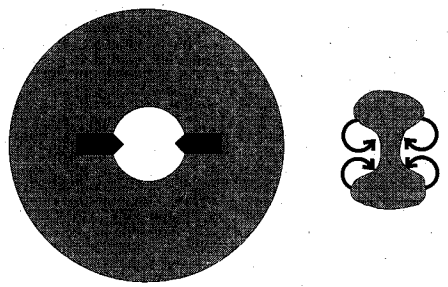

Fig. 2 Sketch of the counter-rotating vortices generated by each tab and the subsequent deformation of the jet.

Another group of measurement techniques currently in use involve a molecular filter, which acts to discriminate Doppler shifted light, in front of the receiving optics. Planar velocity fields have been obtained from particulate scattering in widely varying flow regimes using this approach.[7-9] A closely related diagnostic, filtered Rayleigh scattering, relies on molecular, rather than Mie scattering. Miles et al.[10] and Forkey et al.[11] have measured average velocities and thermodynamic properties across planar fields of a supersonic jet by scanning the laser frequency across the absorption well of an iodine absorption filter and recording multiple images for each frequency setting. A similar approach was taken in the present investigation, but with a narrower scope. Rather than obtaining detailed flow properties, limited quantitative data was gathered from images taken for a single laser frequency.

The ultimate goal of this work was twofold. The first ambition was to better illuminate the effect of tabs on a supersonic jet using a unique visualization technique. The second was to utilize the filtered Rayleigh scattering technique to experimentally verify that tabs generate streamwise vorticity in supersonic jets.

Experimental Setup

The Aeronautical and Astronautical Research Laboratory (AARL) at the Ohio State University, is equipped to handle high pressure and mass flow conditions. Two storage tanks of 42.5 m^3 capacity and capable of withstanding pressure of up to 16.5 MPa (2400 psig) permitted practically unlimited operation of the present experiments.

The plenum chamber has a diameter of 20.2 cm (8 in.), and the maximum operating stagnation pressure was 1.7 MPa (250 psig). Contoured axisymmetric Mach 1.0, 1.5, and 2.0 nozzles, also used in Ref. 12, with an exit diameter of 1.9 cm (0.75 in.) were used throughout the experiments. A 97-kW Watlow air heater capable of withstanding the elevated pressures was available to provide high stagnation temperatures for the FRS experiments.

Dual-view instantaneous flow visualizations were obtained using a pulsed Quanta Ray GCR-4 Nd:YAG laser, and two scientific grade 14-bit Princeton Instruments intensified charge-coupled device (CCD) cameras. The second harmonic of the Nd:YAG (with a wavelength of 532 nm) was split and spread into two perpendicular sheets that were then passed through the flowfield. For the dual-view visualization case, condensed water particles from the moisture present in ambient air served as the marking media in the mixing layer. The two intensified CCD cameras were positioned to capture each illuminated plane.

Each camera was controlled via a Princeton Instruments PG-200 programmable pulse generator that interfaced with the camera controller and the laser. A synchronizing electronic pulse from the laser was transmitted to each controller that subsequently gated each camera. The laser pulsewidth was 9 ns, which effectively freezes the flow. However, the laser pulse repetition rate of 10 Hz was far too slow to capture any real-time data, and the recorded images may be considered random in time from frame-to-frame. The digitized images were directly stored on two 486/33-MHz personal computers and later processed.

In addition to using laser sheet lighting to examine flow features on a qualitative level, quantitative laser diagnostics were utilized to obtain data across an entire plane. This was accomplished using a filtered Rayleigh scattering (FRS) technique. While the flow visualization techniques discussed in the previous text rely on particles in the mixing layer, the quantitative data sought in this case involves only molecular scattering. The effect of dark current on the recorded pixel intensity was negligible since the camera was shot-noise limited.

Unfortunately, it is often difficult to sufficiently eliminate undesired scattering off surfaces and/or particles in the flow. The intensity of scattering from these sources generally dominates the Rayleigh signal. Partly for this reason the filtered Rayleigh scattering technique was developed. Miles et al.[10] scanned the laser frequency through the well of the filter and were able to determine average values for density, temperature, and a velocity component across a plane by analyzing the Rayleigh scattering profile in the frequency domain. This approach to eliminate stray laser light is also useful as a flow visualization technique for unseeded flows where it has been used to study compressible mixing layers and boundary layers.[13,14]

A key component to FRS is an optical cell of gaseous molecules that absorb light at the incident laser frequency while transmitting the Doppler shifted light scattered off molecules moving with the flow. Thus, the incident light scattered off stationary surfaces can be selectively eliminated while the Doppler shifted light is recorded by the camera, and the resultant signal-to-noise ratio is greatly enhanced. A schematic of the experimental setup is provided in Fig. 3.

The camera was fitted with a 90-mm lens, and the f number used was 11. The camera was located 110 cm from the interrogated plane approximately 24.5 deg off the streamwise axis, causing the scattering angle θ to be 114.5 deg. For ambient conditions the resultant y parameter, which will be described later, used to characterize the Rayleigh spectra was 0.71.

The principal reason for using diatomic iodine is that it absorbs light in specific bands near the wavelength of a frequency doubled Nd:YAG (532 nm). Normally, the frequency content of the beam emitted from a Nd:YAG laser would be too broad to use this technique. However, an injection seeder laser may be used to narrow the frequency content of the incident light to within about 50 MHz.[15] A voltage applied to control the temperature of a diode in the seeder laser may then be used to vary the frequency of the laser beam across a range of about 50 GHz.

The filter used in the present work is similar to those used in previous studies.[13-15] The pressure and temperature of the gaseous iodine in the cell can be used to control the filter

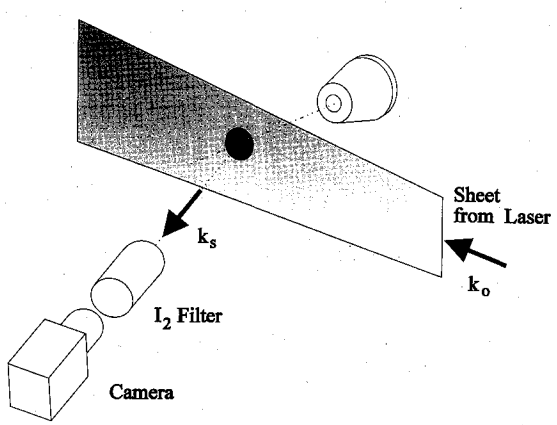

Fig. 3 Sketch of the optical setup for the filtered Rayleigh scattering measurements in supersonic jets. The filter contains diatomic iodine in a gaseous state.

absorption characteristics based on collision and temperature broadening. Elliott et al.[8] discuss these issues, along with filter optimization for different kinds of flow measurements. For the measurements contained in the present work, the water bath surrounding the arm of the filter containing iodine crystals was kept at 40°C. This established how much of the iodine was in the vapor state. The rest of the filter was maintained above this value (approximately 85°C) to ensure that no deposition of iodine occurred on the front or back windows of the cell. No foreign gases were present inside the cell for these experiments. A profile of the filter was obtained by scanning the laser frequency through the iodine absorption bands while collecting light scattered off a surface. More aspects of the filter profile are discussed in the results.

Dual-View Flow Visualization Results

In the subsequent three figures (Figs. 4–6), each pair of front- and side-view images was recorded at the same instant. The front view shows a plane of the jet (x/D = 3) with the flow out of the page, and the side view shows the flow from about x/D = 2 to 4 with the flow moving left to right. The bright line present in each image is actually the laser sheet for the orthogonal view. For each experimental condition a total of 25 pairs of images were recorded, but here only a few samples are displayed. Table 1 provides details about the operating conditions.

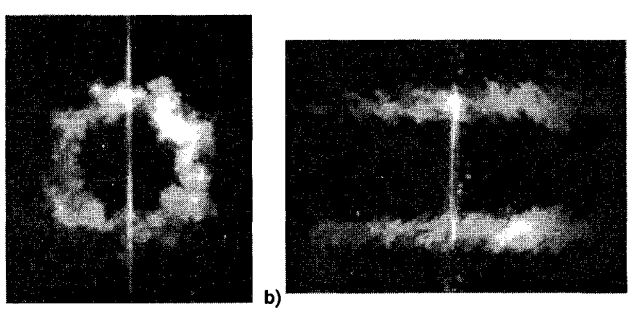

Fig. 4 Dual-view image of a perfectly expanded Mach 1.5 jet without tabs: a) front view (x/D = 3), and b) side view (x/D = 2–4).

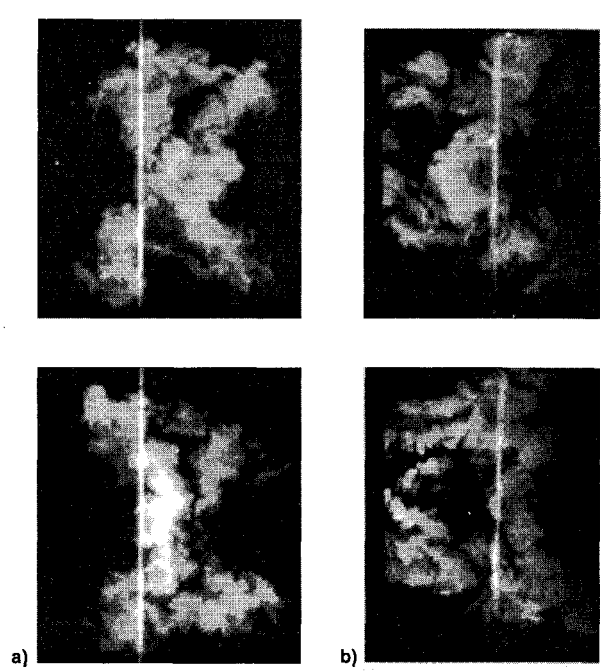

Fig. 5 Dual-view image of a perfectly expanded Mach 1.5 jet with two delta tabs: a) left column shows a front view (x/D = 3) and b) the right column shows a side view (x/D = 2–4).

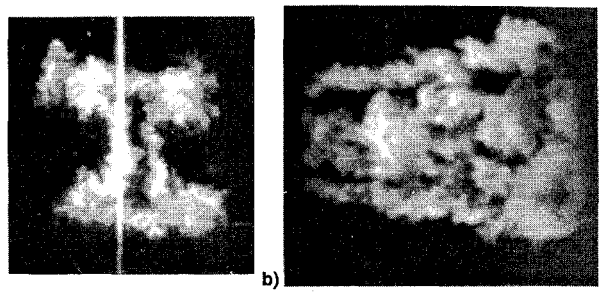

Fig. 6 Dual-view images of a Mach 2.0 perfectly expanded jet with two delta tabs. On the left is a) front view image (x/D = 3), and b) side view (x/D = 2–5).

A Mach 1.5 jet without tabs is shown in a dual-view visualization in Fig. 4. For this case, the convective Mach number calculated from isentropic expansion was 0.67, as shown in Table 1, which is within the regime where compressibility affects the mixing layer to some extent.[16] As indicated by the bright line in the front views, the laser sheet for the side view shows a plane through the center of the jet. The side-view visualization shows mixing layer structures angled toward the jet centerline, as expected. The areas of condensation apparent in the front-view visualization (x/D = 3) appeared to vary in their azimuthal locations from frame-to-frame. The larger areas of condensation around the circumference of the jet are generally indicative of streamwise vortices. Previous studies suggest that these streamwise vortices are spatially stationary for underexpanded jets.[12] However, some variation is not uncommon in perfectly expanded jets emanating from smooth nozzles with a highly turbulent flow.

Two dual-view visualizations of a Mach 1.5 jet with two delta tabs are given in Fig. 5. The front view shows the jet (x/D = 3) such that the tabs extend from the left and right side of the nozzle for each image. The drastic distortion of the jet from each delta tab is consistent with earlier observations.[4] In comparing the front view with the side view (which shows a plane of the mixing layer near a tab from approximately x/D = 2 to 4), structures formed in the layer show some intricate features of the mixing. A number of side-view images revealed large-scale structures within the mixing layer that bridge the bifurcated jet core. The second pair of images is notable in that part of the swept back structure was captured in the front view as well. In the side view, the front view intercepts a portion of a structure at the center of the image. The corresponding front view shows a very strong signal at nearly the same spatial location. These structures are remarkably similar to those seen in low Reynolds number incompressible cases.[5] Given the convective Mach number and turbulence regime of the flow, this is somewhat surprising. In addition, density variations caused by shocks emanating from the tabs make this strong similarity to incompressible cases even more unexpected.

Similar visualizations were performed for a Mach 2 jet. The Mach 2 jet without tabs showed very little variation from the Mach 1.5 case and are given elsewhere.[6,17] Visualizations for a Mach 2 jet with delta tabs showed more interesting results and a typical example is given in Fig. 6. Again from the front view it is clear that the jet is severely distorted by the tabs. The side view shows highly disorganized structures within the flat portion of the mixing layer. This is in contrast to the Mach

Table 1 Flow characteristics for the dual-view supersonic jet experiments

M_j	T_j, K	a_1, m/s	U_1, m/s	U_2, m/s	a_2, m/s	U_c, m/s	M_c
1.5	193	279	418	0	340	230	0.67
2.0	156	250	500	0	340	250	0.85

1.5 delta tab case that intermittently showed structures similar to that of an incompressible jet with tabs. This difference is likely a result of increased compressibility levels for the Mach 2 case.[13] On the other hand, the nature of the distortion of the jet, as viewed from the front, is virtually the same for both cases, consistent with previous observations.[3,4]

Filtered Rayleigh Scattering Results

To interpret the FRS results, it is necessary to understand characteristics of the Rayleigh scattering signal itself. One property of Rayleigh scattering that has been used extensively in flow diagnostics is that the density of an illuminated gas is directly proportional to the intensity of the scattered light. As discussed earlier, such measurements are difficult to perform because of the Rayleigh signal, which is weak in comparison to particulate scattering. When a filter is employed, part of the spectra is blocked. Thus, it is necessary to describe the Rayleigh signal and its relationship to the filter in the frequency domain. The shape of the Rayleigh scattering curve in the frequency domain may be described as a function of temperature, density, and θ. Here, this shape is given as $R^*(f)$. The vertical scale (R^*) is such that

$$I = \rho \int_{f\to-\infty}^{f\to\infty} R^*(f)\, df \tag{1}$$

where the I is an arbitrary intensity level.

The spectra of Rayleigh scattering for ambient conditions ($\rho_\infty = 1.22$ kg/m^3 and $T_\infty = 285$ K) with the viewing angle was computed using the six-moment scheme of Ref. 18. This is shown in relation to the optical filter profile in Fig. 7. This profile was computed by scanning the laser frequency while recording light scattered off a surface. The profile compares well with the computed absorption profile of Forkey et al.[11] The incident laser frequency was held constant to within the limitations of the injection seeder throughout the flow experiments. While constant monitoring of the laser frequency is the preferred approach, the seeder provided excellent repeatability, as evidenced by separate scanned profiles of the filter.

Because some of the scattered light is absorbed by the filter, the recorded intensity would now be described as

$$I_\infty = \rho_\infty \int_{f\to-\infty}^{f\to\infty} [R^*(f_0, \rho_\infty, T_\infty, \theta)][P_{\text{filter}}(f_0)]\, df \tag{2}$$

When the imaged gas is moving relative to the transmitting and receiving optics, the central frequency of the Rayleigh scattering spectra experiences a shift according to the relation:

$$\Delta f = (\bar{V}/\lambda)\cdot(\overline{k_s} - \overline{k_0}) \tag{3}$$

where $\boldsymbol{k}_s$ is the unit vector for the scattered light and $\boldsymbol{k}_0$ is the unit vector corresponding to the incident laser sheet. As one can see from Fig. 7, a positive frequency shift would result in more of the Rayleigh spectra passing through the filter, and a higher measured intensity. This intensity may be described as

$$I = \rho \int_{f\to-\infty}^{f\to\infty} [R^*(f_0 + \Delta f, \rho, T, \theta)][P_{\text{filter}}(f_0)]\, df \tag{4}$$

As with Eq. (2), the intensity would be in arbitrary units. Quantitative data may be obtained by comparing the intensity within the moving flow to the ambient within the same image. Thus, with the intensity ratio I/I_∞ computed across the image, a planar region of the flow may be interrogated.

If the thermodynamic properties of the moving flow are equal to those of the ambient (i.e., $\rho = \rho_\infty$ and $T = T_\infty$), the shape of the Rayleigh scattering spectra would not vary across the image. In such a case, the intensity ratio is solely a function of frequency shift, from which the velocity component in the direction determined by the wavevectors may be found. This approach is the basis for determining the velocity within the isothermal jet without tabs.

In contrast, if the thermodynamic properties of the moving flow are different from the ambient, the velocity component cannot be uniquely determined. From these images, however, the resultant image can be shown to be representative of a value combining thermodynamic properties and a velocity component. This is the approach used to determine quantitative characteristics of the flow for jets with tabs employed at the nozzle exit, where shock waves affect the thermodynamic properties of the flow.

The measured intensity ratio of Doppler shifted to unshifted light may be summarized in the following fashion:

$$\frac{I}{I_\infty} = \frac{\rho}{\rho_\infty} \times D[(\boldsymbol{k}_s - \boldsymbol{k}_0)\cdot\bar{V}] \times E\left(\frac{\rho}{\rho_\infty}, \frac{T}{T_\infty}, \bar{V}\right) \tag{5}$$

The function term D is associated with the Doppler shift. The function E accounts for variations in the shape of the Rayleigh scattering spectra.

The determination of the intensity ratio from an image is a relatively straightforward matter; however, a few considerations must be made. While the filter will eliminate scattering off surfaces, the light scattered by particles moving with the flow still affects the recorded image. Condensation was eliminated as a consequence of heating the flow to cause an iso-

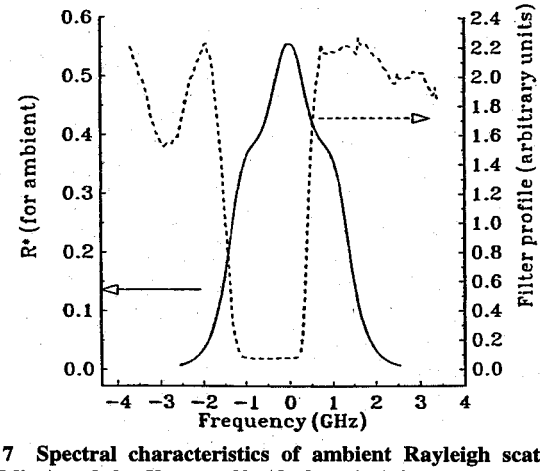

Fig. 7 Spectral characteristics of ambient Rayleigh scattering (solid line) and the filter profile (dashed line) for the experimental setup. Zero frequency refers to the incident frequency of the laser.

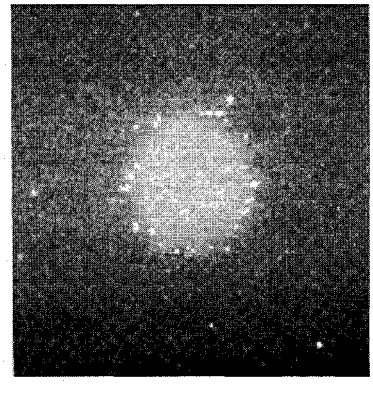

Fig. 8 Typical instantaneous filtered Rayleigh scattering image of a perfectly expanded, isothermal Mach 2 jet without tabs.

thermal jet, but even without the condensation, other particles in the ambient were entrained and appeared intermittently in the images. Nevertheless, a number of relatively clean images were recorded, and the few particles that did appear were eliminated in postprocessing when the images were averaged by excluding the pixels, which exceeded an arbitrarily high intensity threshhold. A typical instantaneous image taken at x/D = 3 for the Mach 2.0 jet without tabs is given in Fig. 8. The bright region in the center of the image is the core of the jet, where the flow causes a positive Doppler shift, and appears elliptical because of the camera angle. The location of the bright particles, seen primarily in the mixing layer, varied from frame-to-frame. All quantitative data were based on an average of 100 images.

Another complicating matter was that the recorded ambient intensity level varied with the spatial location. This is partly because of the Gaussian nature of the laser sheet. Another cause for this is that the distance to the camera lens varied slightly (about 1%) across the image plane because of the viewing angle. These variations were accounted for by a two-

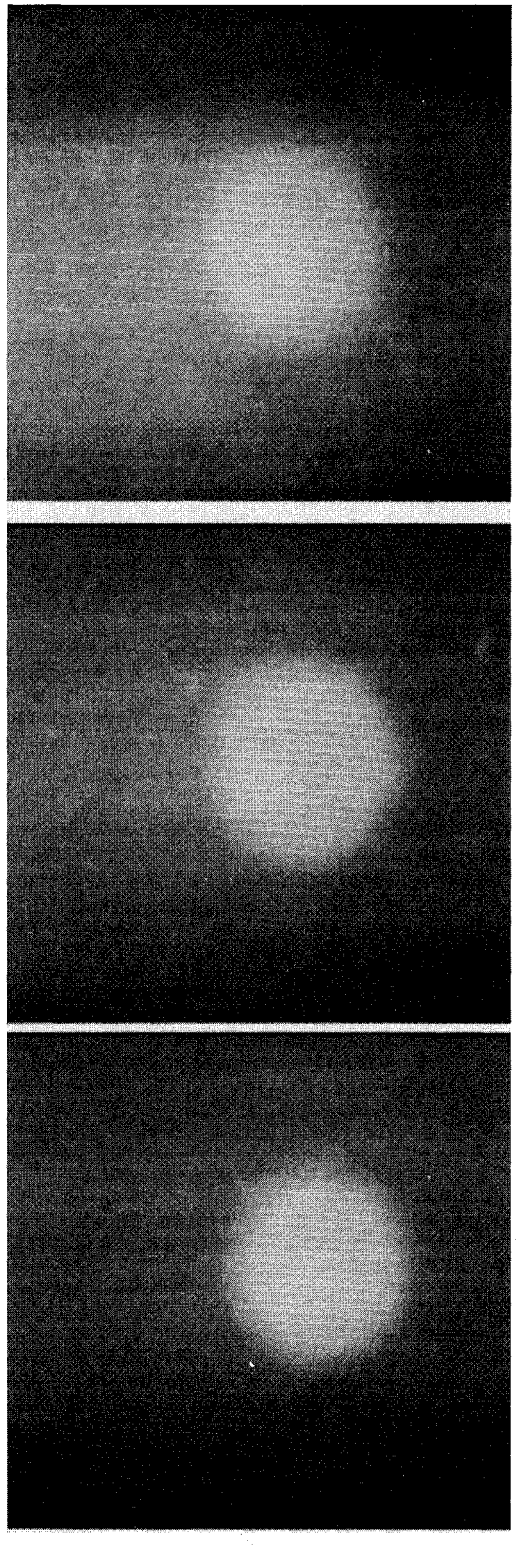

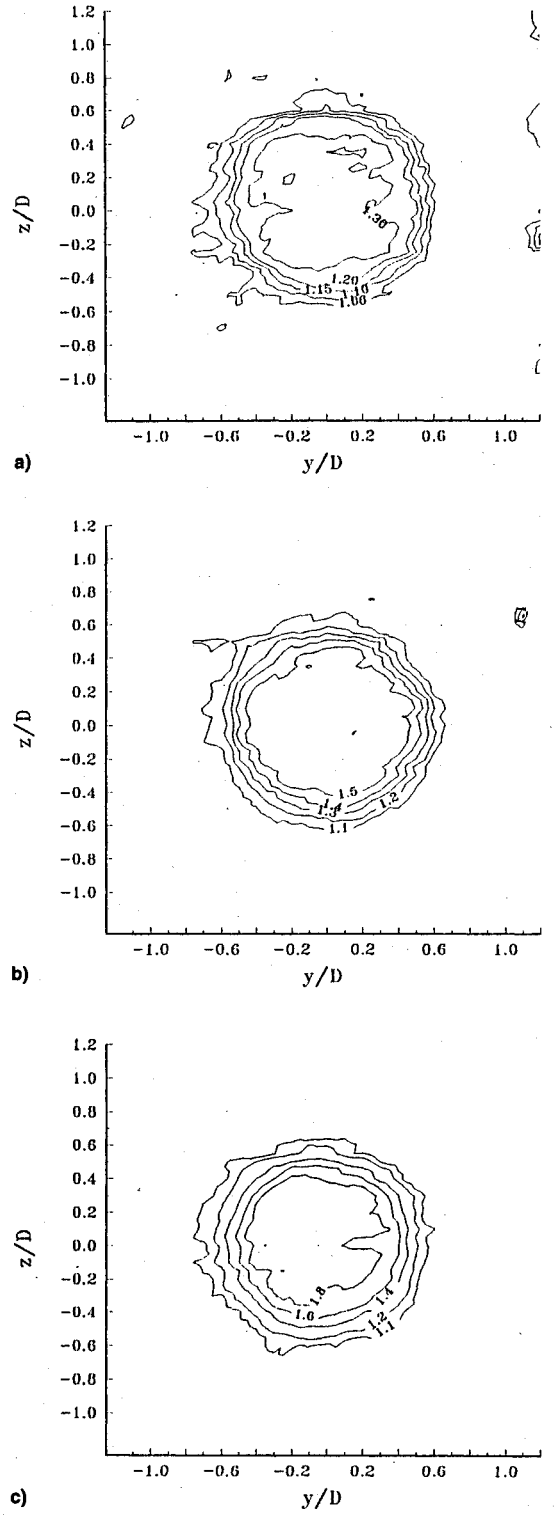

Fig. 9 Postprocessed, average images of filtered Rayleigh scattering are in the left column, and the right column gives intensity ratios for perfectly expanded, isothermal Mach a) 1.0, b) 1.5, and c) 2.0 jets without tabs. Data was taken at x/D = 3 for each case.

dimensional parabolic curve fit based on values for I_∞ well into the ambient of each average image. This generated I_∞ for each pixel from which the intensity ratio was calculated.

Results for Jets Without Tabs

The averaged images for isothermal Mach 1.0, 1.5, and 2.0 jets without tabs taken at $x/D = 3$ are shown in the left-hand column of Fig. 9. It can be seen here that the intensity levels within the jet core relative to the ambient increase as the Mach number is increased for these isothermal jets. This is better expressed by the contour levels of I/I_∞ shown in the right-hand column. The skewness of the camera view is also corrected here using a fine grid recorded by the camera prior to each measurement. These contours were calculated by generating a 50 by 50 array of intensity ratio values from the average images. This was done by choosing regularly spaced y and z points using the grid for calibration. A weighted average of the four pixels intensities surrounding the desired location were used to determine the intensity ratio for each point (i.e., 2500 values of I/I_∞ were calculated for each image). In essence, this is equivalent to taking measurements with a spatial resolution of $0.04D$ in both the y and z directions for a $2.0D$ by $2.0D$ cross section.

Because the jet is pressure and temperature matched, the intensity ratio in the jet is strictly a function of a component of the jet velocity to within experimental error. The component of velocity measured is based on $\boldsymbol{k}_s - \boldsymbol{k}_0$ as demonstrated in Eq. (3). This was $0.91\boldsymbol{i} - 1.41\boldsymbol{k}$. When symmetry about the y axis is assumed, the streamwise component U may be calculated for each case.

The transmission of light through the filter at this incident frequency was used to calculate I_∞ with $P_{\text{filter}}(f)$ representing a scalar value. The intensity was calculated from the filter profile and the scattering curve (both shown earlier in Fig. 7) assuming a shift of Δf from the incident frequency:

$$\frac{I}{I_\infty}(\Delta f) = \frac{\int_{-\infty}^{\infty} R^*(f + \Delta f) P_{\text{filter}}(f)\, df}{\int_{-\infty}^{\infty} R^*(f) P_{\text{filter}}(f)\, df} \tag{6}$$

This calculation, based solely on the calculated Rayleigh scattering spectra and the measured filter profile, was performed for a number of Δf. The way in which Δf varies with I/I_∞ is shown by Fig. 10. It can be seen from this plot that the intensity ratio rises monotonically with the frequency shift. Since the shift in the flowfield is because of the Doppler effect, the velocity in the direction determined by the wavevectors was then calculated directly from the intensity ratio using a fourth-order polynomial curve fit for Δf. Then with the assumption of symmetry about the y axis [i.e., $U(y) = U(-y)$, and $W(y) = -W(-y)$], the streamwise velocity may be found.

The results of the calculation are given in Fig. 11 for Mach 1.0, 1.5, and 2.0 (in Figs. 11a–11c, respectively). Contour lev-

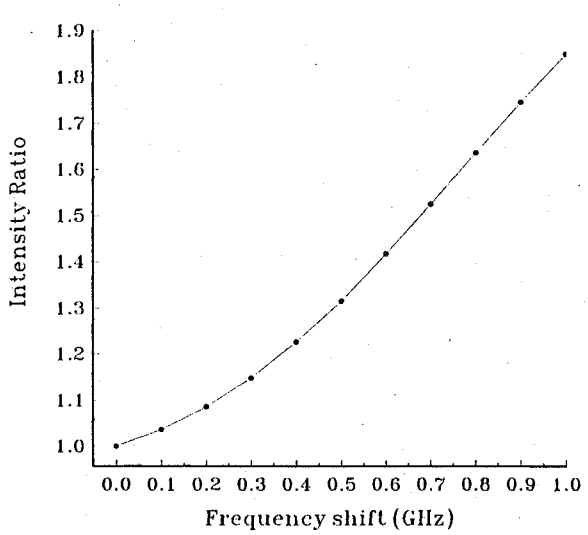

Fig. 10 Relationship between the Doppler shift and intensity ratio, as calculated from the spectra of Rayleigh scattering and the iodine filter shown in Fig. 7.

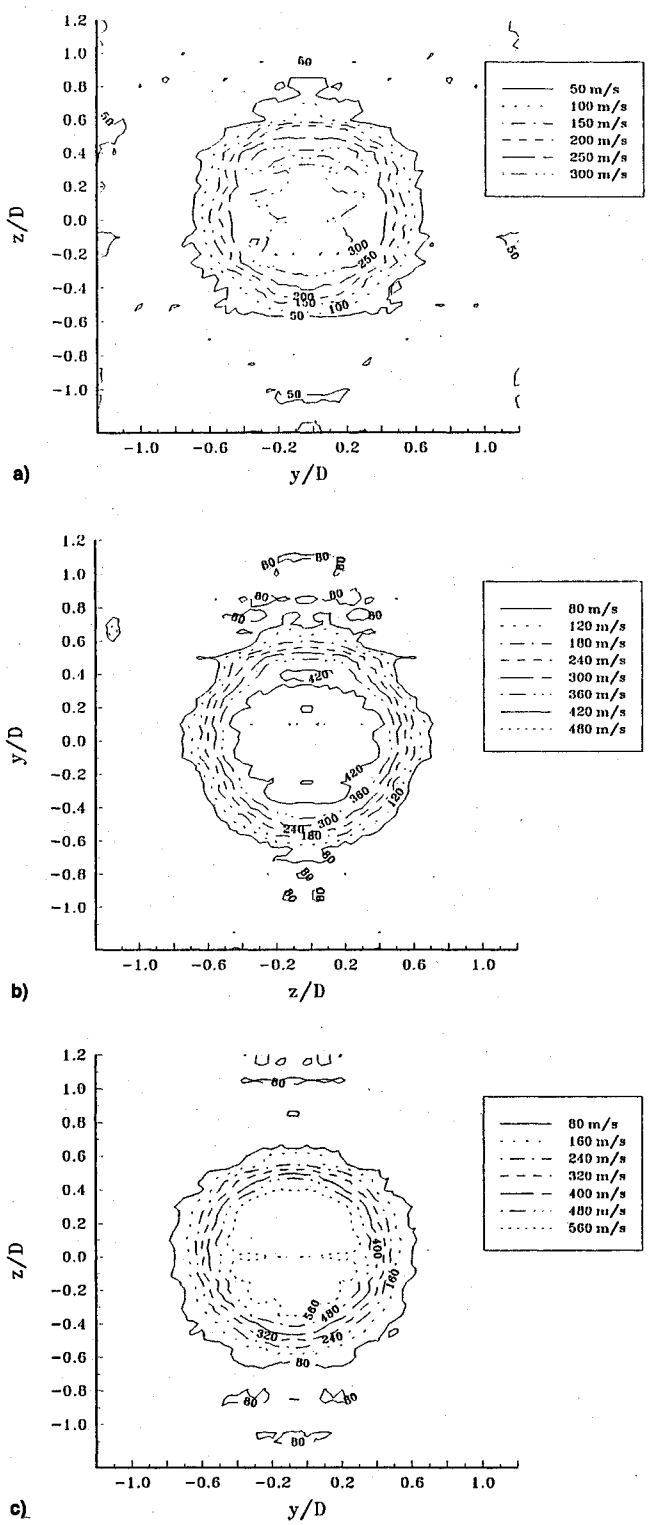

Fig. 11 Streamwise velocities determined from filtered Rayleigh scattering images of isothermal jets without tabs. Data was taken at $x/D = 3$ for Mach a) 1.0, b) 1.5, and c) 2.0 jets.

els are seen to increase for each increment in the Mach number. The trend of increasing velocity is fairly accurately depicted through each jet mixing layer, and increases to higher levels with each increment in jet Mach number. However, the levels in the core of each jet are about 10–15% lower than expected for each case (see Table 2 for expected values), indicating that some error is present.

Among the possible error sources are several that may easily be addressed in future work. The consistently lower-than-expected values for U could be because of an inaccurate assessment of the wavevectors in relation to the streamwise axis of the jet. For instance, if the jet centerline actually passed 4 deg from the x axis (in the negative y direction), the streamwise velocity would appear to increase by 11%. The assumption of isentropic flow would seem to be reasonable for calculating density and temperature from known stagnation conditions, but direct measurement of these values were not obtained. Also, note that these results are based on only 100 images.

Yet another source of error could be that the threshold set to eliminate scattering from particles might have clipped some of the higher instantaneous density or velocity fluctuations inside the jet core. Such an error would reconcile the consistently lower-than-expected velocity measurements. Correcting this source in future measurements could prove more difficult since it would require a better method of filtering particles in the mixing layer. Background white light and dark current are not suspected of causing this error since the camera was shot-noise limited.

Results for Jets with Tabs

When delta tabs are used to perturb the jet, direct measurements of velocity cannot be made using this approach without

Table 2 Flow characteristics for the FRS experiments

D, cm	P_0, MPa, absolute	T_0, K	M_j	T_j, K	ρ_j, kg/m^3	U_j, m/s	$Re_D \times 10^6$	ρ_j/ρ_∞	M_c
1.90	0.1879	335	1.0	279	1.24	335	0.667	1.02	0.50
1.90	0.3647	400	1.5	276	1.25	499	0.992	1.03	0.75
1.90	0.7721	500	2.0	278	1.24	667	1.31	1.02	1.00

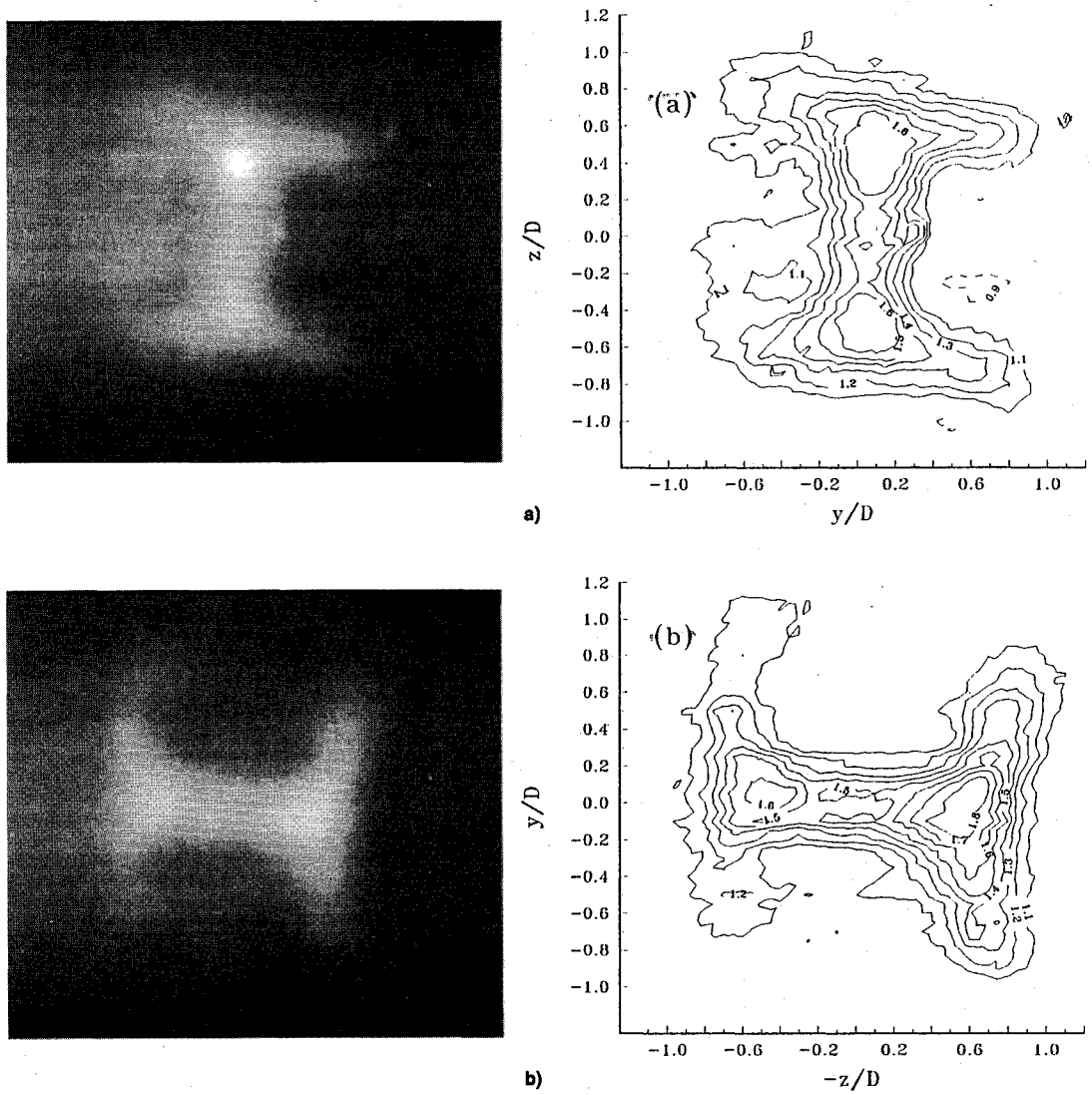

Fig. 12 Postprocessed average-filtered Rayleigh scattering images of a Mach 1.5 jet with two delta tabs and their respective intensity ratios. The tabs are along the a) horizontal axis and b) the vertical axis.

scanning the laser frequency. This is because the shocks that are necessarily generated by the tabs for the supersonic jets result in the density and temperature varying with spatial location. This holds true even though the stagnation temperature was raised such that an isentropic expansion would result in an isothermal flowfield. In terms of Eq. (5) this means that ρ/ρ_∞ and the term denoted E may be nonunity. Still, the signal remains strongly dependent on directional velocity.

Average images for the two-delta-tab Mach 1.5 fully expanded, temperature-matched jet are shown in the left column of Fig. 12. The difference in the setup between Figs. 12a and 12b is the tab orientation (i.e., the tabs enter the flow from the left and right sides in Fig. 12a and from the top and bottom in Fig. 12b). The most obvious feature of this figure is that the jet core is highly distorted compared to the no-tab cases. This is consistent with previous observations. Corresponding intensity ratio contours, spatially corrected for the camera angle, are shown in the right column of Fig. 12. With the camera angle used, the wave vector was $0.91\boldsymbol{i} - 1.41\boldsymbol{j}$ for Fig. 12a and $0.91\boldsymbol{i} - 1.41\boldsymbol{k}$ for 12b. Note that the z axis for Fig. 12b is set negative so that the image in the left column corresponds directly to this intensity ratio.

Pure velocity measurements are obscured by variations in density and temperature, but the intensity ratio still may be interpreted in a quantitative manner. When symmetry is assumed for density and temperature as well as velocity, it is clear from these plots that the tabs generate secondary flow for the supersonic cases. In fact, if the V and W components of velocity were zero, the intensity ratio contours would be symmetric for both of these plots. The asymmetry indicates that the secondary flows are generated.

More direct quantitative information can be gathered when the effect of the E term in Eq. (5) on the FRS signal is assumed to be negligible. The values

$$(I/I_\infty)_{y>0} + (I/I_\infty)_{y<0} = \rho^* \times [2 + 1.82 \times f(U)] \quad (7)$$

$$(I/I_\infty)_{y>0} - (I/I_\infty)_{y<0} = \rho^* \times [2.82 \times f(V)] \quad (8)$$

where ρ^* denotes ρ/ρ_∞ and f denotes a linear approximation of the monotonically increasing function term dependent on a velocity component. This first-order approximation can be made simply by assuming symmetry about the tab axis. Equation (7) is obtained by adding the values of the intensity ratio on either side of the plane of symmetry, whereas Eq. (8) is the result of subtraction. Similarly to this the values

$$(I/I_\infty)_{z>0} + (I/I_\infty)_{z<0} = \rho^* \times [2 + 1.82 \times f(U)] \quad (9)$$

$$(I/I_\infty)_{z>0} - (I/I_\infty)_{z<0} = \rho^* \times [2.82 \times f(W)] \quad (10)$$

can additionally be calculated for the spanwise axis. These calculations were performed, and the values on the right-hand side of Eqs. (7–10) are shown in Figs. 13a and 13b and Figs. 14a and 14b.

There are a few reasons why the assumption of a negligible effect by the E term is a valid approximation for this data. The incident laser frequency was chosen such that the Doppler shift in the higher velocity regions of the jet, which correspond to where one might expect to find the widest variations in temperature, cause the Rayleigh spectra to fall halfway inside the filter. Since the effect of temperature on the Rayleigh scattering spectra is symmetric about the central frequency, it would have little effect in those regions. Even in the lower velocity regions, the spectral width varies only with the square root of temperature. Overall, the maximum expected variation in temperature, based on shock relations, for these cases is likely to vary only by roughly 15% from the no-tab case. An additional error may be present because of the selection of a plane of symmetry. Nevertheless, the general characteristics of the measurements appear to be well represented and consistent.

Confidence in the measurements is provided by the consistent values obtained for the streamwise velocity-related calculations shown in Figs. 13a and 14a. For both the $U-V$ [Eq. (7)] and the $U-W$ [Eq. (9)] related measurements, the contours involving the streamwise component are quite comparable. The W-related contours indicate that the flow is directed outward away from the tab axis while the V-related contours show that the ambient air is being entrained into the core along the tab axis. These results are characteristically similar to those obtained using hot-wire anemometry and LDV in subsonic flows.[4,6] Thus, it is reasonable to conclude that the overall pattern of streamwise vorticity generated is also quite similar to that of the subsonic case depicted in Fig. 2, as expected.

For the Mach 2.0 tab case, the postprocessed averaged images taken at $x/D = 2$ were similar in overall appearance to the Mach 1.5 tab case. However, the magnitude of the intensity ratio for each tab orientation, shown in Fig. 15, was generally higher for the two-delta-tab cases oriented for $U-V$ and $U-W$. It is clear that the intensity ratio values are asymmetric

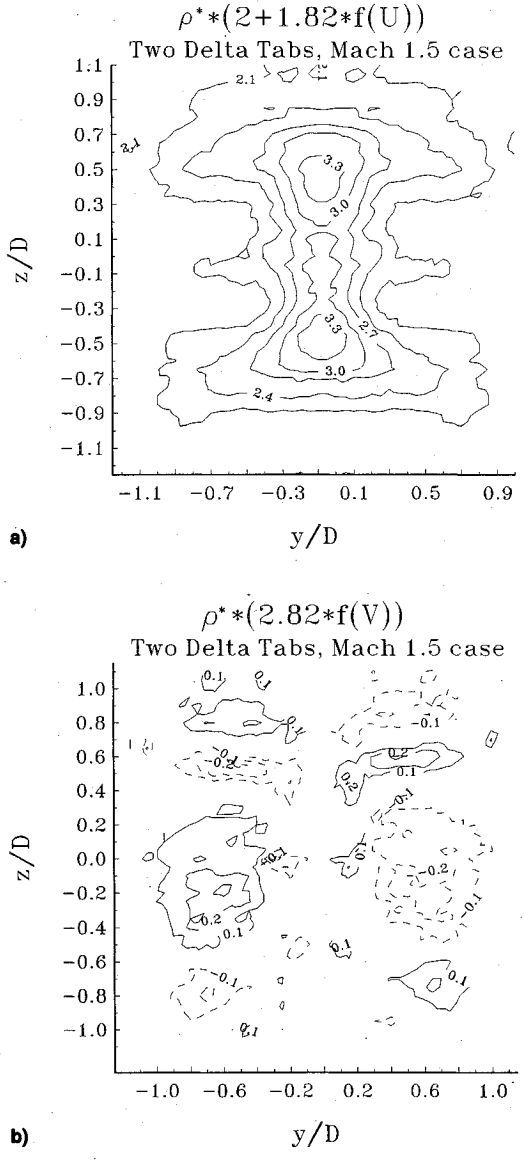

Fig. 13 Quantitative information derived from filtered Rayleigh scattering for a Mach 1.5 jet with tabs (from Fig. 12a). The data is related to a combination of the density ratio and the a) U and b) V components of velocity. Symmetry was assumed about the z axis.

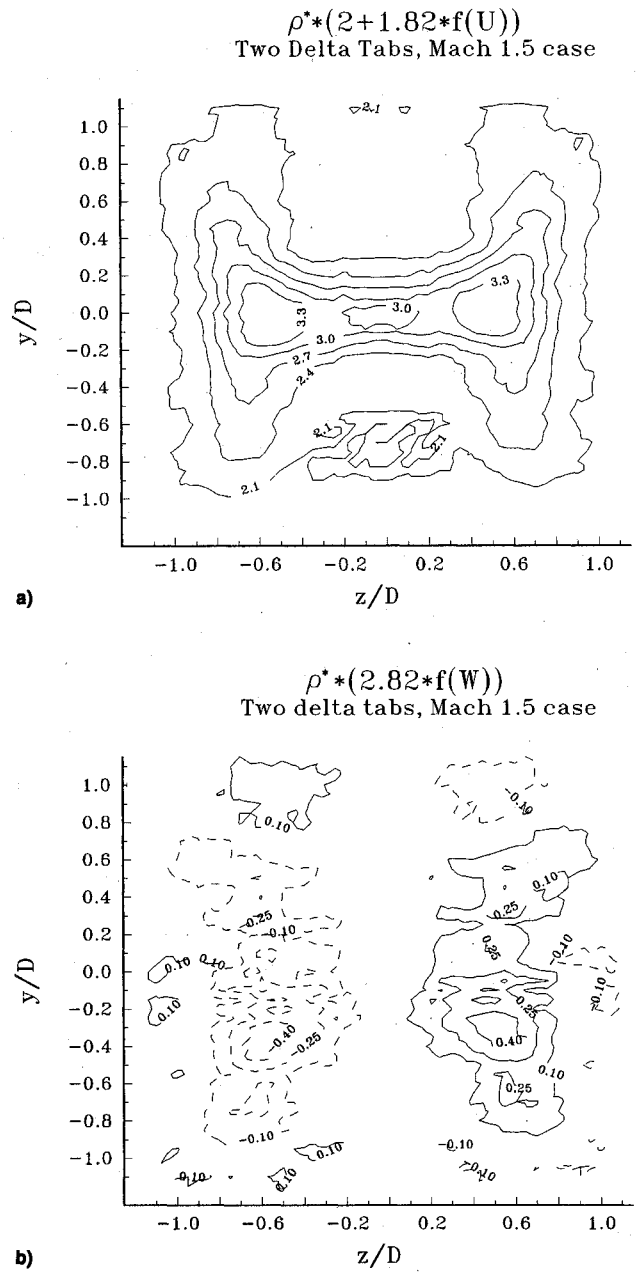

Fig. 14 Quantitative information derived from filtered Rayleigh scattering for a Mach 1.5 jet with tabs (from Fig. 12b). The data is related to a combination of the density ratio and the a) *U* and b) *W* components of velocity. Symmetry was assumed about the *z* axis.

in a fashion similar to that of the Mach 1.5 case, indicating the presence of secondary flow similar to that of subsonic jets with tabs. Equations (7–10) could be applied to this case as well, though larger temperature variation caused by shock strength weakens the assumption of a negligible *E* term. This manipulation of the Mach 2.0 case (proceeding in a similar manner to that described for Mach 1.5) is given elsewhere.[6]

Another notable feature in the intensity ratios for the Mach 2.0 cases is that higher values are seen within the bifurcated cores (about 2.0–2.2) than for the core of the jet without tabs (about 1.8). Upon close inspection, this trend can also be seen for the Mach 1.5 cases. It is virtually certain that this increase is because of density effects. While the density effects cannot be delineated from the velocity using only this data, the images obtained via FRS contain clear and useful quantitative information. Thus, the use of filtered Rayleigh scattering as a diagnostic tool is demonstrated.

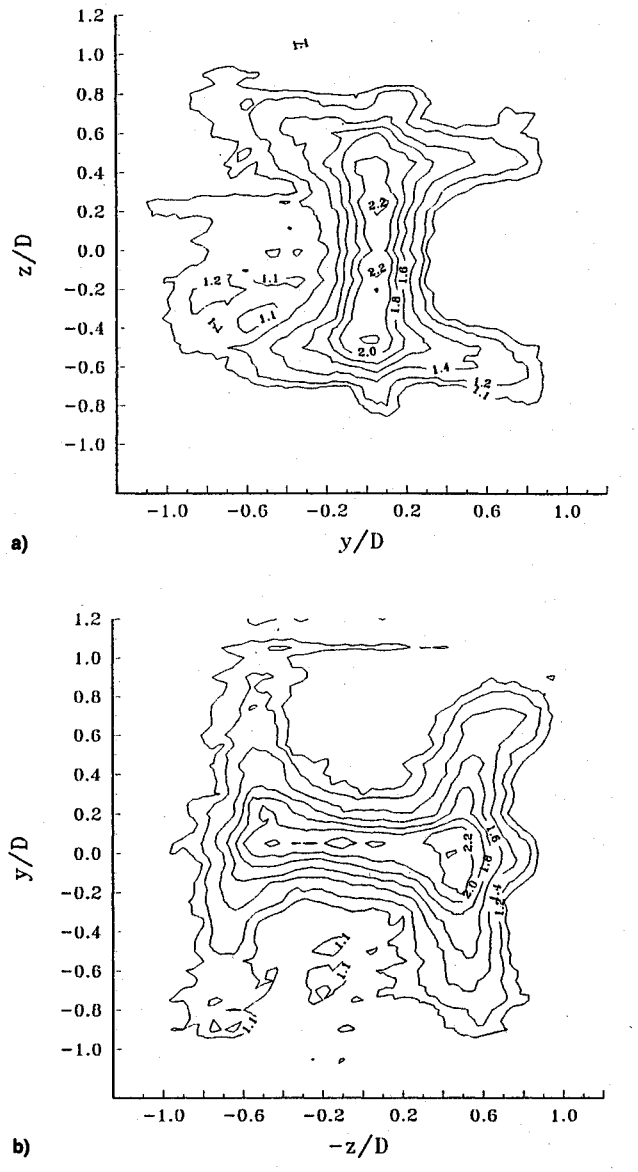

Fig. 15 Processed intensity ratios for a Mach 2.0 jet with two delta tabs. As in Fig. 12, a) the tabs are along the horizontal axis and b) the tabs are along the vertical axis.

Concluding Remarks

The effect of tabs on supersonic jets has been assessed using two unique laser-based experimental techniques. Images of the jet mixing layers have been obtained simultaneously from two orthogonal perspectives, yielding considerable insight into the characteristics of mixing. A marked difference in structure organization was noted for increased compressibility levels in jets both with and without tabs.

Quantitative data were gathered using filtered Rayleigh scattering, a planar-field laser-based diagnostic. By prudently choosing the incident laser wavelength relative to an iodine optical filter and assuming symmetry, streamwise velocities were measured for the specific cases of isothermal Mach 1.0, 1.5, and 2.0 jets without tabs. The measurements yielded generally correct trends, but were somewhat lower than expected values. Potential reasons for the discrepancy are discussed.

When tabs were employed, secondary flows generated by tabs were detected by the FRS method. These indicated the presence of streamwise vortices that were seen in previous work with subsonic jets. Their presence was expected for the supersonic cases as well, but the results given here are the first direct quantitative evidence of their existence.

Acknowledgments

The authors appreciate the support and funding through NASA Grant NAG3-764 with contract monitor Dr. K. B. Zaman. The authors would like to thank Steve Arnette and Vince Belovich for their assistance in performing these experiments and through helpful discussion.

References

[1]Bradbury, L. J. S., and Khadem, A. H., "The Distortion of a Jet by Tabs," *Journal of Fluid Mechanics*, Vol. 70, 1975, pp. 801–813.

[2]Ahuja, K. K., and Brown, W. H., "Shear Flow Control by Mechanical Tabs," AIAA Paper 89-0994, March 1989.

[3]Samimy, M., Zaman, K. B. M. Q., and Reeder, M. F., "Effect of Tabs on the Flow and Noise Field of an Axisymmetric Jet," *AIAA Journal*, Vol. 31, No. 4, 1993, pp. 609–619.

[4]Zaman, K. B. M. Q., Reeder, M. F., and Samimy, M., "Control of an Axisymmetric Jet Using Vortex Generators," *Physics of Fluids*, Vol. 6, No. 2, 1994, pp. 778–793.

[5]Reeder, M. F., and Samimy, M., "The Evolution of a Jet with Vortex-Generating Tabs: Flow Visualization and Quantitative Measurements," *Journal of Fluid Mechanics*, Vol. 311, 1996, pp. 73–118.

[6]Reeder, M. F., "An Experimental Study of Mixing Enhancement in Jets with Vortex Generating Tabs," Ph.D. Dissertation, Ohio State University, Dept. of Mechanical Engineering, Columbus, OH, 1994.

[7]Komine, H., Brosnan, S. J., Litton, A. B., and Stappaerts, E. A., "Real Time, Doppler Global Velocimetry," AIAA Paper 91-0337, Jan. 1991.

[8]Elliott, G. S., Samimy, M., and Arnette, S. A., "Study of Compressible Mixing Layers Using Filtered Rayleigh Scattering Based Visualizations," *Experiments in Fluids*, Vol. 18, 1994, pp. 107–118.

[9]Lee, J. W., Meyers, J. F., Cavone, A. A., and Suzuki, K. E., "Doppler Global Velocimetry Measurements of the Vortical Flow Above an F/A-18," AIAA Paper 93-0414, Jan. 1993.

[10]Miles, R. B., Forkey, J. N., and Lempert, W. R., "Filtered Rayleigh Scattering Measurements in Supersonic/Hypersonic Facilities," AIAA Paper 92-3894, June 1992.

[11]Forkey, J. N., Finkelstein, N. D., Lempert, W. R., and Miles, R. B., "Control of Experimental Uncertainties in Filtered Rayleigh Scattering Measurements," AIAA Paper 95-0298, Jan. 1995.

[12]Arnette, S. A., Samimy, M., and Elliott, G. S., "On Streamwise Vortices in High Reynolds Number Supersonic Axisymmetric Jets," *Physics of Fluids*, Vol. 5, No. 1, 1993, pp. 187–202.

[13]Elliott, G. S., Samimy, M., and Arnette, S. A., "The Characteristics and Evolution of Large-Scale Structures in Compressible Mixing Layers," *Physics of Fluids*, Vol. 7, No. 4, 1995, pp. 864–876.

[14]Arnette, S. A., Samimy, M., and Elliott, G. S., "Structure of Supersonic Turbulent Boundary Layer After Expansion Regions," *AIAA Journal*, Vol. 33, 1995, pp. 430–438.

[15]Elliott, G. S., "A Study of Compressible Mixing Layers Using Filtered Rayleigh Scattering Based Diagnostics," Ph.D. Dissertation, Ohio State Univ., Dept. of Mechanical Engineering, Columbus, OH, 1993.

[16]Samimy, M., and Elliott, G. S., "Effects of Compressibility on the Characteristics of Free Shear Layers," *AIAA Journal*, Vol. 28, No. 3, 1990, pp. 439–445.

[17]Reeder, M. F., Samimy, M., and Elliott, G. S., "An Investigation of the Effect of Tabs on Jets Using Advanced Diagnostics," AIAA Paper 95-0672, Jan. 1995.

[18]Yip, S., and Nelkin, M., "Application of a Kinetic Model to Time-Dependent Density Correlations in Fluids," *Physical Review*, Vol. 135, 1964, A1241–A1245.